

## THEORETICAL STUDIES ON NITRILE-FORMING ELIMINATION REACTIONS\*

IKCHOON LEE,† HYOUNG YEON PARK AND BON-SU LEE

Department of Chemistry, Inha University, Incheon, 402-751, Korea

AND

BYUNG HOO KONG AND BYUNG CHOON LEE

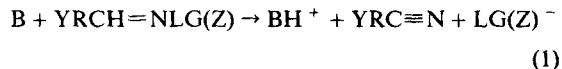
Department of Chemistry, Choongbuk National University, Chongju, 360-763, Korea

The base-promoted nitrile-forming elimination reactions of  $\text{YCH}=\text{CHC}_\beta\text{H}=\text{NOCH}=\text{CHZ}$  ( $\text{Y}=\text{OCH}_3$ ,  $\text{H}$  or  $\text{Cl}$  and  $\text{Z}=\text{H}$  or  $\text{NO}_2$ ) were studied by the AM1 MO theoretical method with  $\text{Cl}^-$  as a base. The reaction is found to proceed by an *E1cB*-like *E2* mechanism in which  $\text{C}_\beta\text{—H}$  bond cleavage is more advanced than  $\text{N—O}$  bond breaking. The *syn*-elimination has a more *E1cB*-like transition state (TS) than the *anti* elimination, which is attributed to the structurally favourable  $n_{\text{N}}\text{—}\sigma^*(\text{C}_\beta\text{—H})$  charge-transfer interaction. An electron-withdrawing  $\text{Y}$  substituent lowers the activation barrier by stabilizing negative charge developed on  $\text{C}_\beta$  in the TS. An electron-withdrawing substituent in the leaving group ( $\text{Z}=\text{NO}_2$ ) tends to enhance the *anti* relative to the *syn* elimination process by depressing the  $\sigma^*(\text{N—O})$  level, which in turn makes the  $n_{\text{C}}\text{—}\sigma^*(\text{N—O})$  interaction more effective. The  $\text{YCH}=\text{CH}^-$  and  $^-\text{C}_\beta\text{H}=\text{N}$  fragments are perpendicular in the TS, which is stabilized by delocalization of negative charge developed on the  $\text{C}_\beta$  atom.

### INTRODUCTION

Bimolecular base-promoted elimination reactions involve a combination of two basic processes:<sup>1–3</sup> removal of a proton  $\beta$  to the leaving group (LG) by a base (B) and breaking of the bond [ $\text{C}_\alpha\text{—LG(Z)}$ ] to the leaving group. The two may take place in a single step (*E2* mechanism) or in two distinct steps; deprotonation occurs first in an *E1cB* elimination, whereas ionization of the LG occurs first in an *E1* elimination. There can be, however, a continuous range of *E2* reactions that are concerted but not synchronous, varying from *E1cB*-like to *E1*-like with a true synchronous *E2*(central) in between (Scheme 1).

The  $\beta$ -eliminations are also common in the base-induced imine<sup>4,5</sup> and nitrile-forming [equation (1)] reactions<sup>6,7</sup>.



where  $\text{Y}$  and  $\text{Z}$  are substituent groups on the substrate

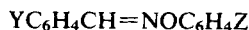
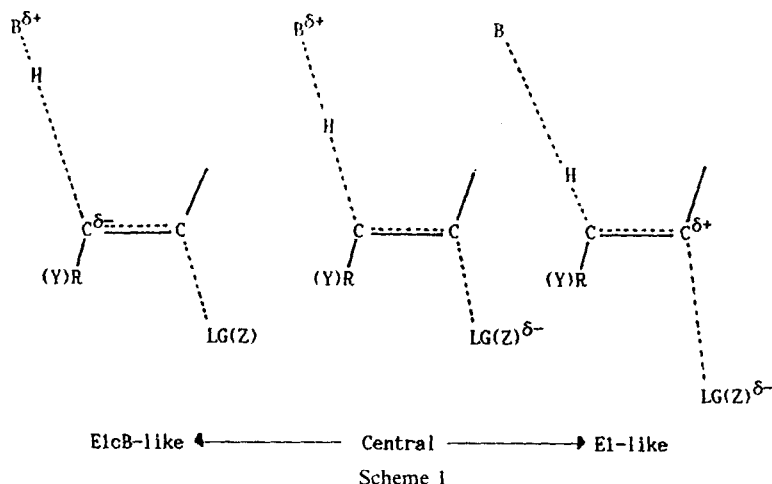
(R) and leaving group (LG), respectively. Although some experimental studies on these have been reported, few theoretical calculations appear to have been carried out,<sup>8,9</sup> and none as far as we are aware on the nitrile-forming elimination by a currently acceptable theoretical procedure. Theoretical calculations are in principle particularly useful for unravelling the problems concerning the timing of bond making and breaking during the  $\beta$ -elimination, which are difficult to solve by experiment.<sup>10</sup>

Here we report our results of AM1 studies<sup>11</sup> on the nitrile-forming eliminations involving effects of substituents in the substrate ( $\text{Y}$ ) and LG( $\text{Z}$ ) on the transition-state (TS) structure.

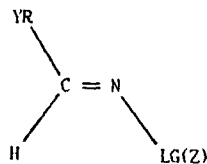
In order to investigate effects of substituents in the substrate and LG, we simplified the *E*- and *Z*-forms of *O*-arylbenzaldehyde oxime, **I**,<sup>10</sup> by substituting an ethylene group for each phenyl ring, **II**<sub>s</sub> and **II**<sub>a</sub>, and varied the substituents  $\text{Y}$  and  $\text{Z}$  ( $\text{Y}=\text{OMe}$ ,  $\text{H}$ , or  $\text{Cl}$  and  $\text{Z}=\text{H}$  or  $\text{NO}_2$ ) with  $\text{Cl}^-$  as a base. In the *E*-form (**II**<sub>s</sub>), deprotonation and LG departure occur in the same

\* Determination of Reactivity by MO Theory, Part 73. Part 72, I. Lee, C. K. Kim, B. H. Kong and B. C. Lee, *J. Phys. Org. Chem.* **4**, 449 (1991).

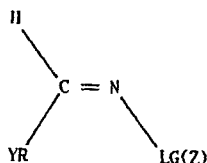
† Author for correspondence.



I



II,

II<sub>a</sub>

direction, a *syn* elimination, whereas in the *Z-form* (II<sub>a</sub>) the two bond-breaking processes take place to the opposite direction, an *anti* elimination. The mechanisms was found to be very similar to that involved in the alkane and imine-forming eliminations, but a lone pair on the nitrogen atom in II<sub>s</sub> and II<sub>a</sub> had a profound effect on the mode of elimination.

### CALCULATIONS

The AM1 procedure<sup>11</sup> was used throughout this work. The reactants and reactant complexes (geometries and energies) were fully optimized with respect to all geometrical parameters and characterized by all positive eigenvalues in the Hessian matrix.<sup>12</sup> TSs were located by the reaction coordinate method,<sup>13</sup> refined by the gradient norm minimization method<sup>14</sup> and characterized by confirming only one negative eigenvalue in the Hessian matrix.<sup>12</sup> The activation entropy,  $\Delta S^\ddagger$ , was obtained by subtracting the calculated entropy of the reactant complex from that of the TS at 298 K, using a program incorporated within the AMPAC.<sup>15</sup>

### RESULTS AND DISCUSSION

#### Reactions with a moderate leaving group (Z = H)

All the reactions had a double-well type of potential energy surface and proceeded through an exothermically formed electrostatic complex (RC) between the base ( $\text{Cl}^-$ ) and substrate (II), which is followed by an activation barrier and a second complex (PC) formed from the products. This means that these reactions occur by the *E2* mechanism so that the proton transfer and the leaving group departure are concerted. This does not mean, of course, that the two bond-breaking processes are synchronous and the degree of bond cleavage in the TS may differ between the two. The TSs for the reactions of II<sub>s</sub> and II<sub>a</sub> are shown in Figure 1.

Inspection of the TS structures reveals that in all cases the proton transfer to the base is much more advanced than the degree of N—O bond cleavage; hence the reactions, irrespective of *anti* or *syn* elimination,<sup>16,17</sup> proceed by the *E1cB*-like *E2* (*E2*/*E1cB*) mechanism. The bond length changes ( $\Delta d$ ) for the C—H, N—O and C=N bonds involved in the activation, i.e.  $\Delta d = d_{\text{TS}} - d_{\text{React}}$ , are summarized in Table 1. As pointed out above,  $\Delta d_{\text{C-H}}$  is by far greater than  $\Delta d_{\text{N-O}}$ , and the bond contraction of the C=N double is also relatively small. Thus, even though the base used in this work,  $\text{Cl}^-$ , is not strong, the nitrile-forming eliminations occur by the *E2*/*E1cB* mechanism. Reference to Table 1 reveals that  $\Delta d_{\text{N-O}}$  is invariably greater for the *anti* elimination and the greater is  $\Delta d_{\text{N-O}}$ , the shorter the C=N bond contracts. This can be rationalized by the charge-transfer interaction involved between the lone pair on N ( $n_{\text{N}}$ ) and the antibonding orbital of the C—H bond ( $\sigma_{\text{CH}}^*$ ), and that between the developing lone pair on C ( $n_{\text{C}}$ ) and the antibonding orbital of the N—O bond ( $\sigma_{\text{NO}}^*$ ) as

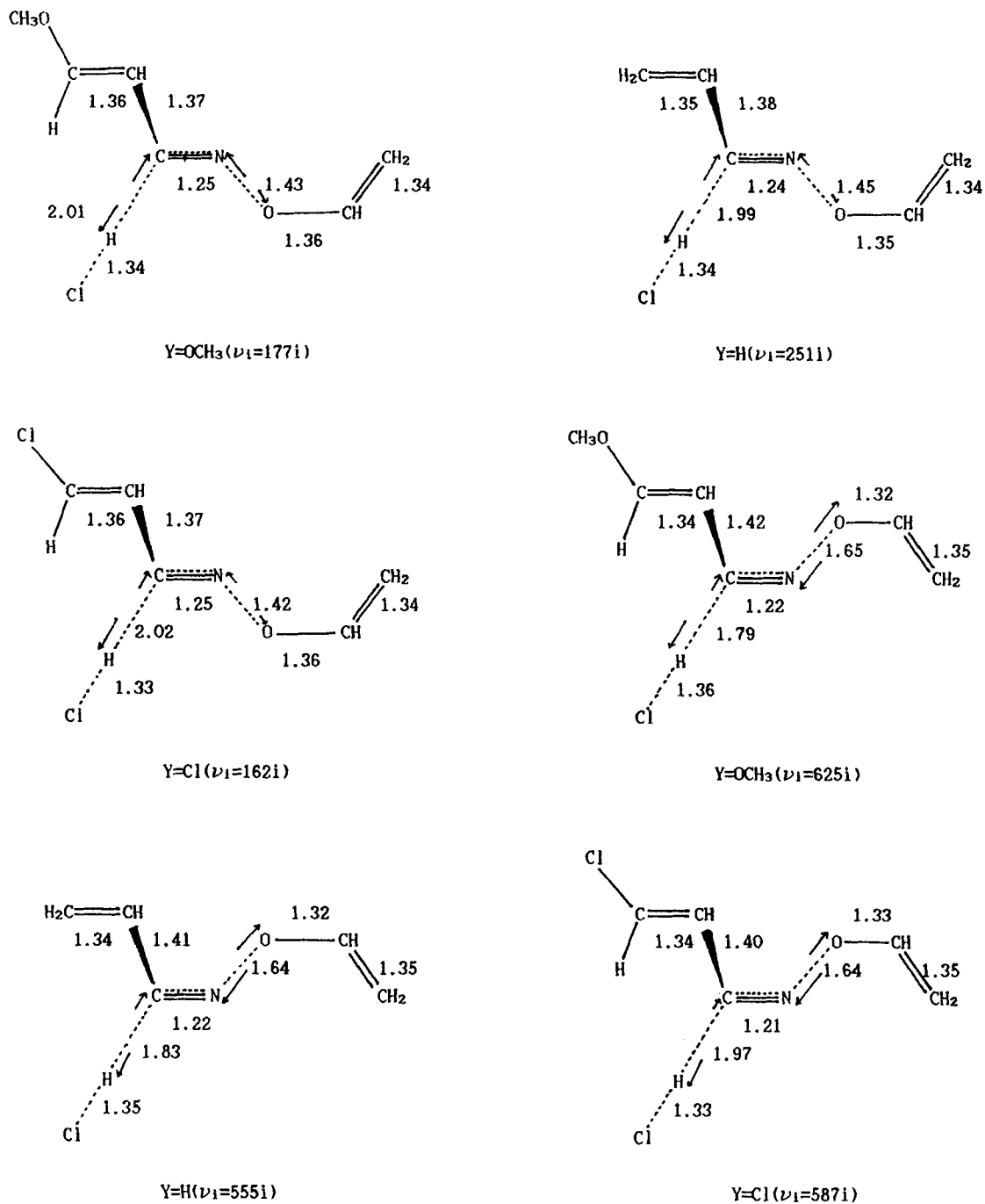
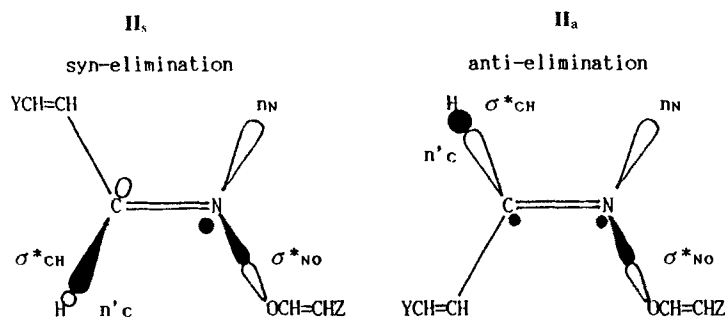


Figure 1. Transition-state structures of *syn* and *anti* elimination, Z = H. Bond lengths in Å; arrows indicate imaginary vibrational modes ( $\nu_i$ s are imaginary frequencies)



Scheme 2

Table 1. Difference in bond length [ $\Delta d(\text{\AA})$ ] between reactant and transition states for  $Z=H$ .

Y	$\Delta d$	<i>syn</i> Elimination	<i>anti</i> Elimination
OMe	$\Delta d_{N-O}$	0.099	0.323
	$\Delta d_{C-H}$	0.903	0.683
	$\Delta d_{C-N}$	-0.061	-0.085
H	$\Delta d_{N-O}$	0.124	0.318
	$\Delta d_{C-H}$	0.876	0.717
	$\Delta d_{C-N}$	-0.064	-0.084
Cl	$\Delta b_{N-O}$	0.094	0.314
	$\Delta d_{C-H}$	0.906	0.854
	$\Delta d_{C-N}$	-0.058	-0.086

shown in Scheme 2. The *syn* elimination is more favourable for the proton abstraction by the base, since charge transfer of the N lone pair ( $n_N$ ) toward the antibonding  $\sigma$  orbital of the C—H bond ( $\sigma_{CH}^*$ ) in the *syn* elimination will be greater with the *anti*-periplanar arrangement between the two compared with the *syn*-periplanar  $n_N-\sigma_{CH}^*$  interaction in the *anti* elimination (Scheme 2).

A greater charge-transfer stabilization by the more efficient  $n_N-\sigma_{CH}^*$  interaction should lead to an earlier TS, i.e. the TS is reached at a lesser C—H bond stretching (smaller  $\Delta d_{CH}$  in Table 1), since the principles of narrowing of inter-frontier level separation and of growing frontier-electron density along the reaction path require a lesser degree of bond breaking for securing a sufficient frontier-orbital density needed to

cross over the activation barrier.<sup>18,19</sup> For  $Y = \text{OCH}_3$ , a greater negative charge at the carbon centre due to the electron-donating effect of the methoxy group should lead to a repulsive interaction with the neighbouring  $n_N$ , which will grow with the proton abstraction, so that a lesser degree of bond breaking seems to be favoured at the TS for the *anti* elimination.

The efficient charge transfer of the N lone pair to the  $\sigma_{CH}^*$  may well be the major factor leading to a relatively large C—H bond scission in the TS with a large *E1cB* character in the *syn* eliminations. Deprotonation having proceeded to a much greater extent in each TS, the partial anionic electron pair formed ( $n_C^-$ ) on  $C_\beta$  can be transferred to the  $\sigma_{NO}^*$  orbital and accelerate the N—O bond cleavage. Now the  $n_C^--\sigma_{NO}^*$  interaction is *anti*-periplanar in the *anti* elimination, so that the N—O bond breaking will be more facilitated compared with the *syn* elimination involving the *syn*-periplanar  $n_C^--\sigma_{NO}^*$  interaction. This is why we have a greater degree of N—O bond breaking in the *anti* elimination. A greater degree of N—O bond breaking will result in a greater degree of  $\pi$ -bond formation, leading to a partial triple bond,  $C\equiv N$ , in the TS; since deprotonation is facile and proceeds to a much greater extent, the  $C\equiv N$  bond formation is largely dependent on the less advanced bond breaking of the N—O bond. Since deprotonation occurs to a greater extent in the TS than ionization of the LG, the negative charge development on  $C_\beta$  is greater than that on O (Table 2).

The dihedral angle between the two fragments,  $YCHV=CH-$  and  $-C_\beta H=N-$ , is almost  $90^\circ$ , as can be seen in the TS structures presented in Figure 1,

Table 2. Charge development in the activation ( $\Delta q = q_{TS} - q_{\text{Reactant}}$ ) in electron units for  $Z = H$ .

Y	$C-1$		$C_\beta$		$N_\alpha$		O(in LG)	
	<i>syn</i> Elim.	<i>anti</i> Elim.	<i>syn</i> Elim.	<i>anti</i> Elim.	<i>syn</i> Elim.	<i>anti</i> Elim.	<i>syn</i> Elim.	<i>anti</i> Elim.
OMe	-0.334	-0.150	-0.407	-0.360	0.167	0.177	-0.246	-0.237
H	-0.260	-0.149	-0.423	-0.345	0.095	0.157	-0.124	-0.244
Cl	-0.257	-0.145	-0.408	-0.353	0.084	0.161	-0.100	-0.235

Table 3. Heats of formation ( $\Delta H_f$ ) of the reactant, reactant complex (RC) and transition state (TS), and enthalpies ( $\Delta H^*$ ), entropies ( $\Delta S^*$ ) and Gibbs free energies ( $\Delta G^*$ ) of activation for  $Z = H$ 

Y	$\Delta H_f$ (kcal mol <sup>-1</sup> )						$\Delta S^{*a}$ (cal mol <sup>-1</sup> K <sup>-1</sup> at 298K)						$\Delta G^{*a}$ (kcal mol <sup>-1</sup> )	
	Reactant		RC		TS		$\Delta H^*$ (kcal mol <sup>-1</sup> )		$\Delta S^*$		$\Delta G^*$			
	<i>syn</i> Elim.	<i>anti</i> Elim.	<i>syn</i> Elim.	<i>anti</i> Elim.	<i>syn</i> Elim.	<i>anti</i> Elim.	<i>syn</i> Elim.	<i>anti</i> Elim.	<i>syn</i> Elim.	<i>anti</i> Elim.	<i>syn</i> Elim.	<i>anti</i> Elim.	<i>syn</i> Elim.	<i>anti</i> Elim.
OMe	-31.26	-33.23	-44.60	-48.58	-27.05	-31.39	17.55	17.19	1.91	7.03	16.98	15.10		
H	14.07	12.38	0.83	-2.67	16.92	12.00	16.09	14.69	0.25	5.27	16.01	13.12		
Cl	3.85	1.96	-12.36	-16.29	0.66	-2.12	13.02	14.17	0.22	5.79	12.95	12.45		

<sup>a</sup> Activation parameter = TS - RC.

owing to the large negative charge development on  $C_\beta$  in the TS. The negative charge developed on the  $C_\beta$  atom delocalizes toward  $HYC^1=CH-$ , forming an allyl anion-type resonance structure. This results in an increase in negative charge on C-1 in the TS, as shown in Table 2.

Despite the negative charge dispersal in the TS, however, charge on  $C_\beta$  is still relatively large (Table 2). This is in line with the relatively large Hammett  $\rho$  values (*ca* 2.0) found in the solution-phase nitrile-forming eliminations of (*E*)-benzaldehyde *N,N,N*-trimethylhydrazonium iodide<sup>20</sup> and (*E*)-oxime ethers.<sup>10</sup> Again, the negative charge development on the oxygen atom is in general greater for the *anti* elimination, indicating a relatively greater degree of bond breaking in the TS for the *anti* than for the *syn* elimination as a result of the more efficient  $n_C-\sigma_{NO}^*$  interaction.

The relevant thermodynamic data obtained by AM1 are given in Table 3. The activation barriers ( $\Delta G^\ddagger$ ) are seen to decrease in general, and hence the reactivity will increase, with an increase in the electron-withdrawing power of substituent Y, in agreement with the experimental results for (*E*)-O-arylbenzaldehyde oxime<sup>10</sup> and (*E*)-benzaldehyde *N,N,N*-trimethylhydrazonium iodides in solution.<sup>20</sup>

The activation barriers ( $\Delta G^\ddagger$ ) are lower for the *anti* elimination of *Z*-isomers (**II<sub>a</sub>**) than for the *syn* elimination of *E*-isomers (**II<sub>s</sub>**). This is consistent with a general trend observed in *E2* elimination reactions that *anti* elimination is more favourable than *syn* elimination.<sup>7</sup> The activation enthalpy,  $\Delta H^\ddagger$ , for Y = Cl is, however, lower for the *syn* rather than for *anti* elimination. This should result from the greater  $n_N-\sigma_{CH}^*$  interaction in **II<sub>s</sub>** in contrast to the greater contribution of  $n_C-\sigma_{NO}^*$  interaction in **II<sub>a</sub>**. The greater  $n_N-\sigma_{CH}^*$  interaction will give a more *E1cB*-like TS structure to **II<sub>s</sub>** owing to a relatively more advanced  $C_\beta-H$  bond cleavage with little N—O bond breaking. In the more *E1cB*-like TS, negative charge development on  $C_\beta$  will be greater, which is more effectively stabilized by a more electron-withdrawing group (Y = Cl) in the *syn* elimination.

On the other hand, the entropy factor,  $\Delta S^\ddagger$ , is seen to be more favourable (Table 3) for the *anti* elimination. This seems to reflect the entropy change involved correctly, since N—O bond breaking is greater in the *anti* elimination whereas proton abstraction by base with  $C_\beta-H$  bond cleavage is more advanced in the *syn* elimination; in the former (N—O bond breaking only) entropy should be gained ( $\Delta S^\ddagger > 0$ ), whereas in the latter (proton abstraction by a base) the entropy change should be small ( $\Delta S^\ddagger \approx 0$ ) since one bond is formed while another bond is broken concertedly. The greater effect of  $\Delta S^\ddagger$  on the *anti* elimination is enough to reverse the reactivity trend in favour of the *anti*-elimination for Y = Cl, for which *syn* elimination is more favoured based on  $\Delta H^\ddagger$ . The more favourable

*anti* elimination found in this work is in agreement with the experimental results for nitrile-forming eliminations of oxime ethers in water-dioxane mixtures.<sup>7</sup>

#### Reaction with a better leaving group ( $Z=NO_2$ )

The nitrile-forming eliminations from **II<sub>a</sub>** and **II<sub>s</sub>** with a better LG,  $Z = NO_2$ , are in general similar to those with a moderate LG,  $Z = H$ , but there are also some significant differences. The bond length changes,  $\Delta d$ , and thermodynamic data involved with  $Z = NO_2$  are summarized in Tables 4 and 5, respectively, and the TSs are presented in Figure 2.

The TS structures shown in Figure 2 are similar to those for  $Z = H$  in Figure 1 except that the extents of  $C_\beta-H$  and N—O bond breaking are relatively smaller, especially for the *anti* elimination. However, examination of Table 4 reveals that in the *syn* elimination the extent of deprotonation is relatively smaller and ionization of the LG has progressed slightly further in comparison with those for the case when  $Z = H$  (Table 1). This means that the TSs for the *syn* elimination with a better LG shift toward the centre in the potential energy surface (PES) diagram (Figure 3). This can be rationalized with the lowering of both  $n_N$  and  $\sigma_{NO}^*$  levels by the electron-withdrawing group,  $Z = NO_2$ . This lowering of levels will result in the less efficient *anti*-periplanar  $n_N-\sigma_{CH}^*$  interaction (less  $C_\beta-H$  bond cleavage) and the more efficient *syn*-periplanar  $n_C-\sigma_{NO}^*$  interaction (greater N—O bond breaking). The latter interaction ( $n_C-\sigma_{NO}^*$ ) is substantially less efficient leading to less N—O bond breaking in the *anti* elimination because of insufficient development of the  $n'_C$  lone pair due to a less efficient *syn*-periplanar  $n_N-\sigma_{NH}^*$  interaction.

The AM1 bond orders (*P*) for the C—H and N—O bonds are near unity ( $P_{CH} \approx P_{NO} \approx 1.0$ ) for all reactants, and will vanish when the bonds are completely broken. The progress of reaction at the TS will therefore be inversely related to the bond orders. The

Table 4. Difference in bond length [ $\Delta d(\text{\AA})$ ] between reactant and transition state for  $Z = NO_2$

Y	$\Delta d$	<i>syn</i> Elimination	<i>anti</i> Elimination
OMe	$\Delta d_{N-O}$	0.175	0.191
	$\Delta d_{C-H}$	0.531	0.488
	$\Delta d_{C=N}$	-0.062	-0.063
H	$\Delta d_{N-O}$	0.128	0.186
	$\Delta d_{C-H}$	0.619	0.498
	$\Delta d_{C=N}$	-0.055	-0.062
Cl	$\Delta b_{N-O}$	0.160	0.176
	$\Delta d_{C-H}$	0.550	0.569
	$\Delta d_{C=N}$	-0.059	-0.063

Table 5. Heats of formation ( $\Delta H_f$ ) of the reactant, reactant complex (RC) and transition state (TS), and enthalpies ( $\Delta H^*$ ), entropies ( $\Delta S^*$ ) and Gibbs free energies ( $\Delta G^*$ ) of activation for  $Z=\text{NO}_2$ 

Y	$\Delta H_f$ (kcal mol <sup>-1</sup> )						$\Delta S^{*a}$ (cal mol <sup>-1</sup> K <sup>-1</sup> at 298K)						$\Delta G^{*a}$ (kcal mol <sup>-1</sup> )	
	Reactant		RC		TS		$\Delta H^*$ (kcal mol <sup>-1</sup> )		$\Delta S^*$					
	<i>syn</i> Elim.	<i>anti</i> Elim.	<i>syn</i> Elim.	<i>anti</i> Elim.	<i>syn</i> Elim.	<i>anti</i> Elim.	<i>syn</i> Elim.	<i>anti</i> Elim.	<i>syn</i> Elim.	<i>anti</i> Elim.	<i>syn</i> Elim.	<i>anti</i> Elim.	<i>syn</i> Elim.	<i>anti</i> Elim.
OMe	-32.63	-34.41	-56.95	-60.78	-47.57	-56.27	9.38	4.51	0.10	5.16	9.35	2.97		
H	13.22	11.25	-11.68	-15.04	-4.83	-12.81	6.95	2.23	-0.75	0.49	7.07	2.08		
Cl	3.63	1.91	-24.01	-27.75	-18.36	-25.85	5.65	1.90	-0.89	1.58	5.92	1.43		

<sup>a</sup> Activation parameter = TS - RC.

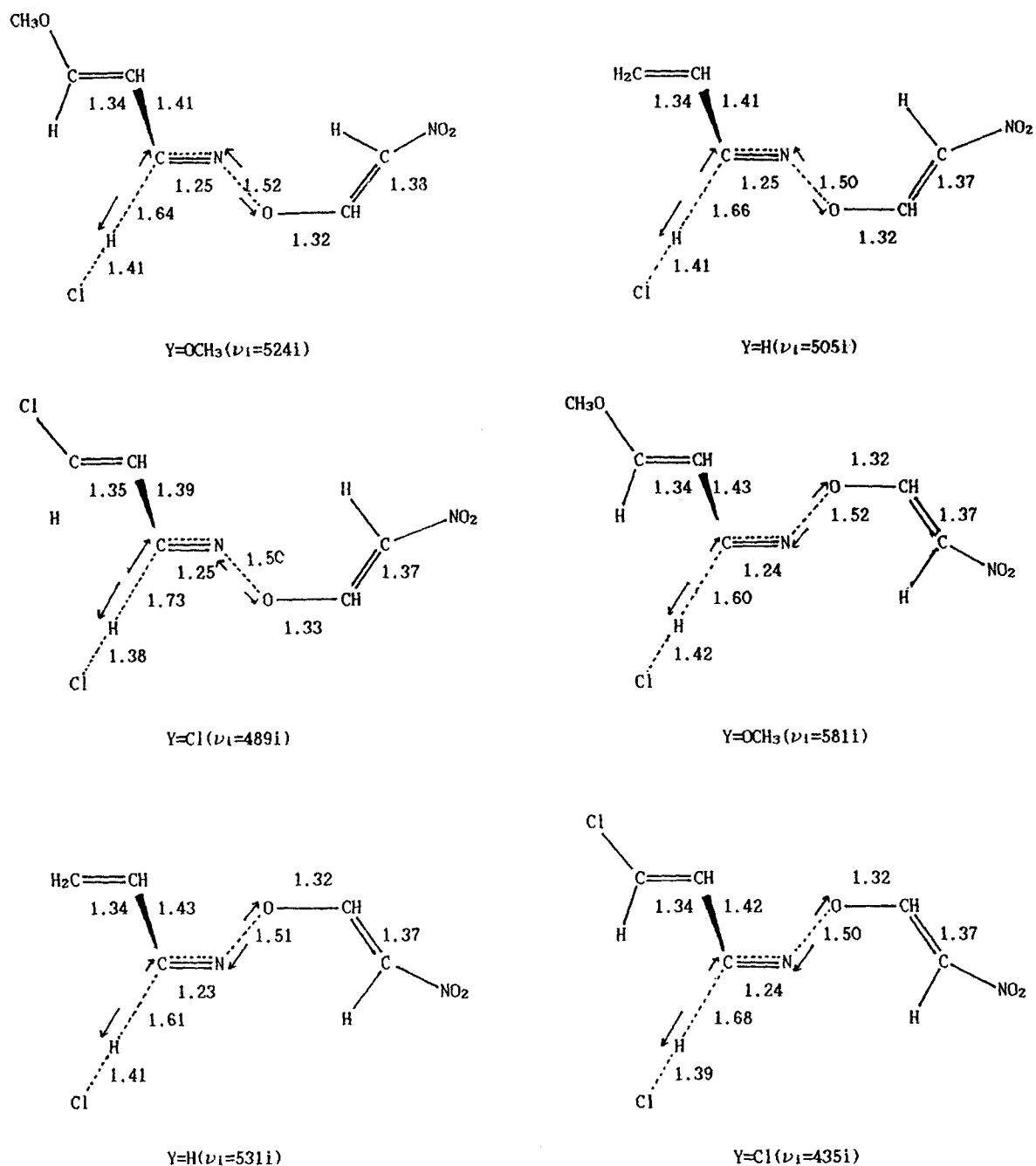


Figure 2. Transition-state structures of *syn* and *anti* elimination,  $Z = \text{NO}_2$ . Bond lengths in Å; arrows indicate imaginary vibrational modes ( $\nu_i$ s are imaginary frequencies)



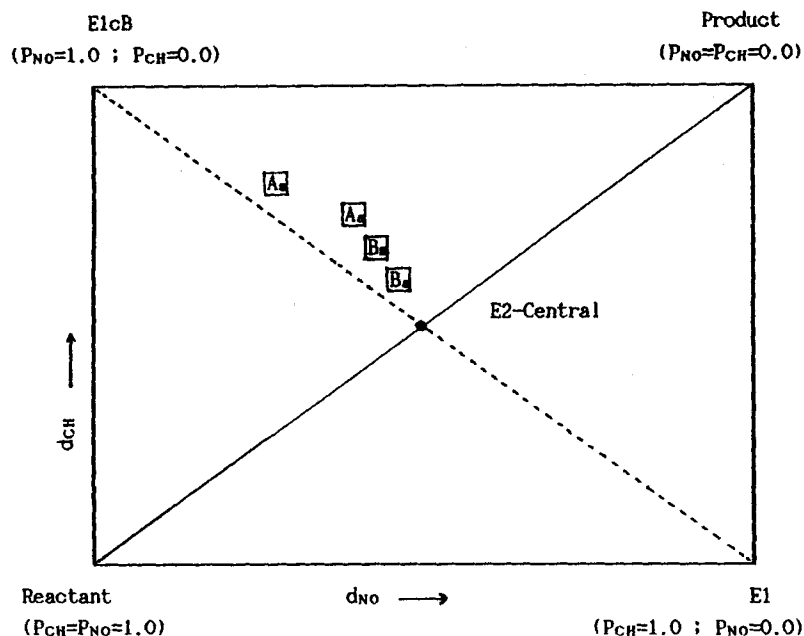


Figure 3. PES diagram for nitrile-forming eliminations with a moderate LG (A; Z = H) and a better LG (B; Z = NO<sub>2</sub>). Subscripts *s* and *a* denote *syn* and *anti* elimination processes, respectively

average percentage change in the bond orders calculated at the TS for  $P_{\text{NO}}:P_{\text{CH}}$  are 26:94 (*syn*) and 49:92 (*anti*) with Z = H and 30:84 (*syn*) and 38:71 (*anti*) with Z = NO<sub>2</sub>. These are shown in the PES diagram in Figure 3. We note that the *syn* elimination with a moderate LG, Z = H, (A<sub>s</sub> in Figure 3) is the most *E1cB*-like whereas the *anti* elimination with a better LG, Z = NO<sub>2</sub>, (B<sub>a</sub> in Figure 3) is the nearest to *E2*-central, and hence a better LG and *anti* elimination are conducive to the *E2* character of the reaction.

The activation barriers ( $\Delta G^\ddagger$ ) in Table 5 indicate that *anti* eliminations are more favoured than *syn* eliminations, similarly to the more favourable *anti* elimination with Z = H. Also, as in the case with Z = H, the activation barrier ( $\Delta H^\ddagger$  and  $\Delta G^\ddagger$ ) is lowered by a more electron-withdrawing Y substituent in all cases, i.e. for both II<sub>a</sub> and II<sub>s</sub>. Furthermore, the activation barriers are lower for both II<sub>a</sub> and II<sub>s</sub> with Z = NO<sub>2</sub> than with Z = H (Tables 3 and 5). This can be attributed, again, to the lowering of the  $\sigma_{\text{NO}}^*$  level by the Z = NO<sub>2</sub> group, leading to a greater contribution of the  $n_{\text{C}}-\sigma_{\text{NO}}^*$  interaction.

Finally, the imaginary frequencies ( $\nu_i$ , in wavenumbers) given in Figures 1 and 2 are seen to be relatively smaller for the II<sub>s</sub> with Z = H. This reflects correctly the most *E1cB*-like TS for the II<sub>s</sub> with Z = H, since the distance  $d(\text{C}_\beta-\text{H})$  is the longest and hence the force constant is the weakest for this case.

We conclude that the nitrile-forming elimination with

a moderate leaving group proceeds by *anti* elimination. This preference is mainly dictated by the relative importance of the *anti*-periplanar  $n_{\text{N}}-\sigma_{\text{CH}}^*$  and  $n_{\text{C}}-\sigma_{\text{NO}}^*$  interactions. In all cases, the reaction proceeds with an *E2/E1cB*-type mechanism. The *E1cB* character increases with an electron-withdrawing substituent in the substrate, whereas the *E2* character increases with a better leaving group.

#### Supplementary materials

Optimized reactant and reactant complex geometries are presented as supplementary materials together with vibrational frequencies of the TS in wavenumbers, and are available from the authors on request.

#### ACKNOWLEDGEMENT

We thank the Ministry of Education for support of this work.

#### REFERENCES

1. D. J. Cram, F. D. Greene and C. H. Depuy, *J. Am. Chem. Soc.* **78**, 790 (1956).
2. J. F. Bunnet, *Angew. Chem., Int. Ed. Engl.* **1**, 225 (1962).
3. R. A. Bartsch and J. F. Bunnet, *J. Am. Chem. Soc.* **90**, 408 (1968).

4. (a) R. V. Hoffman and R. Cadena, *J. Am. Chem. Soc.* **19**, 8226 (1977); (b) R. V. Hoffman and E. L. Belfore, *J. Am. Chem. Soc.* **101**, 5687 (1979); (c) R. V. Hoffman and E. L. Belfore, *J. Am. Chem. Soc.* **104**, 2183 (1982).
5. (a) W. Hanhart and C. K. Ingold, *J. Chem. Soc.* **997** (1927); (b) E. D. Houghes and C. K. Ingold, *Trans. Faraday Soc.* **37**, 658 (1941).
6. R. J. Craford and C. Woo, *Can. J. Chem.* **43**, 1534 (1956).
7. A. F. Hegarty and P. J. Touhey, *J. Chem. Soc., Perkin Trans. 2* 1313 (1980).
8. M. J. S. Dewar and Y. Yuan, *J. Am. Chem. Soc.* **112**, 2095 (1990).
9. M. J. S. Dewar and Y. Yuan, *J. Am. Chem. Soc.* **112**, 2088 (1990).
10. B. R. Cho, J. C. Lee, N. S. Cho and K. D. Kim, *J. Chem. Soc., Perkin Trans. 2* 489 (1989).
11. M. J. S. Dewar, E. G. Zoebish, E. F. Healy and J. J. P. Stewart, *J. Am. Chem. Soc.* **107**, 3902 (1985).
12. I. G. Csizmadia, *Theory and Practice of MO Calculations on Organic Molecules*, p. 239. Elsevier, Amsterdam (1976).
13. (a) K. Muller, *Angew. Chem.* **19**, 1 (1980); (b) S. Bell and J. S. Crighton, *J. Chem. Phys.* **80**, 2464 (1984).
14. (a) J. W. McIver and A. Kormornicki, *Chem. Phys. Lett.* **10**, 303 (1971); (b) J. W. McIver and A. Kormornicki, *J. Am. Chem. Soc.* **94**, 2625 (1972).
15. Program No. 506, Quantum Chemistry Program Exchange (QCPE) Indiana University.
16. R. D. Bach, R. C. Badger and T. J. Lang, *J. Am. Chem. Soc.* **101**, 2845 (1979).
17. T. Minato and S. Yamabe, *J. Am. Chem. Soc.* **110**, 4586 (1988).
18. K. Fukui, *Theory of Orientation and Stereoselection*, pp. 25–30. Springer, Berlin (1975).
19. I. Lee, *J. Chem. Soc., Perkin Trans. 2* 943 (1989).
20. M. T. Nguyen, K. F. Clarke and A. F. Hegarty, *J. Org. Chem.* **55**, 6177 (1990).